

High-resolution profiles and nitrogen isotope tracing reveal a dominant source of nitrous oxide and multiple pathways of nitrogen gas formation in the central Arabian Sea

Joanna Claire Nicholls, Christian Andrew Davies,¹ and Mark Trimmer²

School of Biological and Chemical Sciences, Queen Mary, University of London, London E1 4NS, United Kingdom

Abstract

The oxygen minimum zone (OMZ) of the Arabian Sea is a significant source of nitrous oxide (N₂O), yet the metabolism responsible for N₂O production is unclear. High-resolution profiles identified peaks and troughs of N₂O and NO₂⁻ in the top 500 m of the water column. The first peak in N₂O was not in the oxycline, but deeper at the oxic–suboxic interface. Peaks and troughs were targeted with a suite of ¹⁵N incubations (¹⁵NO₃⁻, ¹⁵NO₂⁻, ¹⁵NH₄⁺) to identify pathways of N₂O and N₂ formation. With ¹⁵NO₂⁻, ¹⁵N-N₂O was produced at all depths with a binomial distribution with respect to the NO₂⁻ pool. With ¹⁵NO₃⁻, the ¹⁵N was not binomially distributed. NO₃⁻ is first reduced to NO₂⁻ before reduction to N₂O, and NO₂⁻ → N₂O is the dominant metabolism responsible for N₂O production. The N₂O produced from ¹⁵NH₄⁺ represented 2–5% of that from ¹⁵NO₂⁻ at the top of the OMZ. In addition, the production of ⁴⁵N₂O, but no ⁴⁶N₂O, at some depths with ¹⁵NH₄⁺, suggested a novel source akin to *Nitrosomonas* spp. under O₂ limitation. Unlike N₂O, the production of N₂ with ¹⁵NO₂⁻ or ¹⁵NO₃⁻ was not binomially distributed and therefore was not entirely derived from the same source as N₂O. Although indicative of an alternative N₂ source to denitrification, the lack of significant production of labeled N₂ with ¹⁵NH₄⁺ discounts anaerobic ammonium oxidation (anammox), as we understand it. Dissolved organic nitrogen or nitrate/nitrite reduction to ammonium are suggested as the additional sources of N in N₂ production.

Large areas of the surface waters of the global ocean are at equilibrium with respect to N₂O and the atmosphere, but regions that are oxygen deplete are significant sources of N₂O (Elkins et al. 1978). The Arabian Sea is one such important source, which is estimated to contribute to between 5% and 18% of the total oceanic N₂O emission (Law and Owens 1990; Naqvi and Noronha 1991). Nitrous oxide is an important atmospheric trace gas, contributing to global warming, ozone depletion, and acid rain formation (Stein and Yung 2003). Although the constraints on the global N₂O budget have improved in recent years, the mechanisms of the major sinks and sources have not yet been fully resolved (Stein and Yung 2003).

In the classic nitrogen (N) cycle, N₂O is formed as an intermediate of denitrification, i.e., facultative anaerobic respiration with NO₃⁻ or NO₂⁻: NO₃⁻ ⇒ NO₂⁻ ⇒ NO ⇒ N₂O ⇒ N₂. Denitrification is dependant on low oxygen concentration (hypoxia), or complete anoxia, and is coupled to the oxidation of organic carbon (Tiedje 1988). In contrast, N₂O is formed as a byproduct of autotrophic nitrification under low oxygen, i.e., NH₄⁺ ⇒ NH₂OH ⇒ (NO ⇒ N₂O) ⇒ NO₂⁻ ⇒ NO₃⁻ (Hynes and Knowles 1978). Data for both

N₂O and O₂ distributions in the Arabian Sea (Law and Owens 1990; Naqvi and Noronha 1991) consistently indicate increasing levels of hypoxia in the productive subsurface waters (0–150 m), along with increasing saturations of N₂O. This is followed by an oxygen minimum zone (OMZ) of varying thickness (200–1000 m), of either extreme hypoxia or complete anoxia, and oxygen begins to rise again below 1000–1200 m. The supersaturation of N₂O in the first 150 m has been linked to the nitrification of NH₄⁺ along the oxycline, and nitrification is considered by some to be the dominant source (Elkins et al. 1978; Codispoti et al. 1992 and references therein; Dore et al. 1998). While this offers one explanation, the observed δ¹⁵N of N₂O (~+7–8‰) from these waters is much higher than that expected for N₂O formed during nitrification, i.e., <–60‰ relative to NH₄⁺, and the issue has been disputed (Yoshida 1988; Kim and Craig 1990; Dore et al. 1998). Naqvi et al. (1998) argue several possible modes of N₂O production in the ocean, involving different isotopic fractionations. Alternatively, a great deal of discussion has focused on denitrification in the ocean, and, indeed, the Arabian Sea is considered to account for one-third of the global water column denitrification (Naqvi 1987), despite it never being measured directly, and actual measurements of denitrification in other open waters being comparatively scarce (Elkins et al. 1978; Brettar and Rheinheimer 1992; Castro-González and Farías 2004). Denitrification activity in an OMZ has largely been inferred from either the presence of a secondary NO₂⁻ maxima, calculated from a NO₃⁻ deficit, or inferred from electron transport system (ETS) activity within oxygen-depleted waters (Deuser et al. 1978; Codispoti and Packard 1980). Technically, though, since NO₃⁻ reduction, which is common to many bacteria, does not produce any gas, it is not denitrification (Tiedje 1988). Within the OMZ, NO₂⁻

¹ Present address: Institute of Ecology, University of Georgia, Athens, Georgia, 30602.

² Corresponding author (m.trimmer@qmul.ac.uk).

Acknowledgments

We thank the crew and technicians on board the R.R.S. *Charles Darwin* and J. Petersen for help with sampling and analysis at sea. We also thank the anonymous reviewers and the associate editor for their helpful suggestions and comments to improve this manuscript. This research has been supported by a Natural Environment Research Council grant (NER/A/S/2001/01196) to M.T.

minima are invariably associated with N_2O maxima and vice versa; hence, denitrification may act as both a sink and a source of N_2O (Codispoti and Christensen 1985; Yoshida et al. 1989; Kim and Craig 1990). Overall, although several decades of research have focused on the role of both nitrification and denitrification in the formation of oceanic N_2O , including that in the Arabian Sea, which process actually dominates or whether a coupling of the two via nitric oxide (NO) potentially could be responsible remains to be resolved (Naqvi et al. 1998).

The confusion over the production of N_2O in the Arabian Sea and other OMZ in the ocean may in part be due to a combination of both low-resolution water column profiles (>50–100 m between sampling points) and a reliance on the interpretation of profile, rather than experimental, data (see review by Codispoti et al. 1992). Though the application of ^{15}N isotope techniques was used to confirm denitrification in the ocean some 40 yr ago (Goering and Dugdale 1966; Wada and Hattori 1972), only very recently has the full potential of ^{15}N isotopes been realized and used to quantify pathways of N_2 formation in open water (Dalsgaard et al. 2003; Kuypers et al. 2003, 2005). More importantly, this later research proved that the novel anammox metabolism, in addition to classic denitrification, was responsible for substantial N_2 production in the OMZ regions of the Golfo Dulce, the Black Sea, and the Benguela upwelling (Dalsgaard et al. 2003; Kuypers et al. 2003, 2005). Hence, N cycling in the global ocean is no longer the sole domain of either nitrification or denitrification. In effect, the way in which we view the N cycle in both pelagic and benthic systems is being revised (Dalsgaard et al. 2005).

The main aims of this study were to better characterize peaks and troughs of N_2O and NO_2^- in the upper 500 m of the Arabian Sea, using high-resolution profiles (10 m), and then to identify pathways for N_2O and N_2 formation by subsequently targeting these depths with a suite of ^{15}N -isotope incubations ($^{15}\text{NO}_3^-$, $^{15}\text{NO}_2^-$, $^{15}\text{NH}_4^+$).

Methods

Water column profiles—Water was sampled within the OMZ of the Arabian Sea during the monsoon in June/July and the intermonsoon period in October/November 2003 at two sites. Site 1 at 20°N 65°E and site 2 at 15°N 65°E , which correspond roughly to N5 and S11 from the US Joint Global Ocean Flux Study (JGOFS) Arabian Sea Process Study (Morrison et al. 1999). Owing to the weather and time constraints on the first cruise, the majority of detailed process measurements were made during the second cruise. A standard conductivity–temperature–depth (CTD) rosette system, comprising of 24 Niskin (10 liter) bottles and Seabird/General Oceanics electronics (fluorimeter, altimeter, par and oxygen sensors, etc.) was used to identify the OMZ and to collect water samples at 10-m intervals between 25 and 500 m. The oxygen sensors had a detection limit of about $0.1 \text{ mL O}_2 \text{ L}^{-1}$ ($\sim 4.5 \mu\text{mol L}^{-1}$).

Nitrous oxide and inorganic nitrogen profiles—Nitrous oxide concentrations were measured by subsampling water

from a Niskin bottle into the bottom of a serum bottle (125 mL) and then allowing it to overflow at least three times before sealing it (aluminum over butyl rubber with polytetrafluoroethylene (PTFE) liners, Chromacol). A headspace (2 mL, analytical grade helium) was then introduced using a two-way valve and gas-tight syringe (SGE Gastight Luer Lock syringe; Alltech Associates). The serum bottles were then shaken vigorously (2 min) and placed on rollers (Spiramix) to allow N_2O to equilibrate between the water phase and headspace at 20°C for at least 2 h. Samples of the headspace (50 μL) were then injected manually using a gas-tight microliter syringe (Vici Precision Sampling) into an Agilent 6890 μ electron capture detector (μECD) gas chromatograph, fitted with both water and CO_2 traps and a Porapak Q column (Upstill-Goddard et al. 1996). The μECD was operated at 350°C with an argon–methane carrier gas (50 mL min^{-1} , 95% Ar, 5% CH_4). Calibration was performed with standards prepared from N_2O (98 ppm; Scientific and Technical Gases). Nitrous oxide concentrations and saturation in the water samples were back-calculated from the measured headspace concentration according to Weiss and Price (1980), adjusted for salinity, air pressure, and temperature, accordingly.

Concentrations of NO_3^- and NO_2^- were measured using a segmented flow autoanalyzer (Skalar) and standard colorimetric techniques (Kirkwood 1996) in further subsamples of unfiltered water (60 mL) collected in acid-washed PTFE bottles. The limits of detection and precision for NO_3^- and NO_2^- were 0.1 and $0.05 \mu\text{mol L}^{-1} \pm 1\%$, respectively. Submicromolar NH_4^+ measurements were made at site 2 on the second cruise using a Turner Designs fluorimeter and the method of Holmes et al. (1999). The fluorimeter NH_4^+ assay had a detection limit of $0.0125 \mu\text{mol L}^{-1} \pm 4\%$.

^{15}N -isotope incubation experiments, ^{15}N - N_2O —The ^{15}N - N_2O production experiments were carried out in triplicate at four depths in October 2003. Following high-resolution profiling, ^{15}N incubation experiments were targeted at depths where NO_2^- and N_2O covaried. Water was sampled using the CTD, as above, and then allowed to flow from a Niskin bottle into the bottom of calibrated volumetric flasks (2 liters), which were allowed to overflow by three times their volume, as above, and then capped. The flasks were then secured in a box and placed in a constant temperature (20°C) laboratory and allowed to acclimatize for 24 h. The 2-liter flasks were then uncapped; enriched to $10 \mu\text{mol L}^{-1}$ for each ^{15}N isotope and their respective analogues by addition from concentrated stocks of $^{15}\text{NO}_2^-$ with $^{14}\text{NH}_4^+$, $^{15}\text{NH}_4^+$ with $^{14}\text{NO}_2^-$, $^{15}\text{NO}_3^-$ with $^{14}\text{NH}_4^+$, and $^{15}\text{NH}_4^+$ with $^{14}\text{NO}_3^-$ (200 μL of degassed [20 min with oxygen-free nitrogen] 100 mmol L^{-1} stocks: ^{15}N isotopes [99.3 ^{15}N atom %] Sigma-Aldrich); and incubated for 96 h. Additional flasks were collected as reference samples to determine the natural abundance of $^{45}\text{N}_2\text{O}$ and $^{46}\text{N}_2\text{O}$ at each targeted depth.

Gases in the 2-liter flasks were then equilibrated in a loop of helium using a modified gas equilibration manifold based on the design of Upstill-Goddard et al. (1996). The equilibration loop was fitted with Swagelok Ultra Torr

fittings, so that a gas sample bulb (125 mL, compatible with the cryofocusing unit) could be placed in line and a sample of gas collected for later in-house analysis by cryofocusing and continuous flow isotope ratio mass spectrometry (*see below*). Briefly, an equilibration frit was secured in the neck of a 2-liter flask and sealed, then a helium headspace (400 mL) was introduced and circulated (10 L min⁻¹, Charles Austin Pumps) in a continuous loop for 20 min. After equilibration, the valves on the gas sample bulb were closed and the sample stored.

On return to the home laboratory, the gas sample bulbs were placed in line with a trace gas preconcentrator unit (PreCon, Thermo-Finnigan). The PreCon flushes the sample bulbs with analytical grade helium, and the gases are then dried and scrubbed of most of the CO₂. The sample is then cryofocused twice in liquid N₂ before final separation of N₂O from CO₂ on a PoraPLOT Q capillary column. The sample is then passed to the continuous flow isotope ratio mass spectrometer (Finnigan MAT Delta^{Plus}, Thermo-Finnigan) via an interface (ConFlo III Interface, Thermo-Finnigan) and the mass charge ratios for *m/z* 44, *m/z* 45, and *m/z* 46 (⁴⁴N₂O, ⁴⁵N₂O, and ⁴⁶N₂O) measured. Calibration is performed with known amounts of N₂O (98 ppm; Scientific and Technical Gases) over the range 0.41 to 13.25 nmol N₂O (Σ ⁴⁴N₂O, ⁴⁵N₂O, and ⁴⁶N₂O) and is linear between 0.8 to 99 pmol for ⁴⁵N₂O and ⁴⁶N₂O. Here, for clarity, we refer to ¹⁵N labeled N₂O as ⁴⁵N₂O and ⁴⁶N₂O and not ²⁹N₂¹⁶O and ³⁰N₂¹⁶O.

¹⁵N-N₂—At each of the targeted depths, at each site, additional Niskin bottles were filled and used for a parallel suite of more detailed ¹⁵N-N₂ gas production experiments. Again, as above, the water was first subsampled into volumetric flasks and sealed. The equilibration manifold was then used to push water out through a dedicated line (2 mm Teflon tubing), under an anaerobic atmosphere, into the bottom of gas-tight vials (Exetainer, 12 mL, Labco), which were then overflowed, sealed, and left to acclimatize for 24 h, as above. This is essentially the same procedure used by Dalsgaard et al. (2003) to measure anammox and denitrification in the water column of Golfo Dulce, but we did not degas the water in the flasks with helium first. Hence, both the ¹⁵N-N₂O and ¹⁵N-N₂ incubations were carried out at as close to ambient oxygen saturations as possible. This also provides a stable natural abundance N₂ baseline and provides a carrier of natural abundance ¹⁴N-N₂O for the ¹⁵N-N₂O analysis. The gas-tight vials were then enriched, as above, by injecting concentrated isotope stocks through the septa of each vial (Hamilton). During the first cruise, a simple dose response (¹⁵N atom %) experiment was carried out at site 2 for each isotope at four depths over 96 h, just to test whether we could measure ¹⁵N enrichment in the N₂ pool. Nitrite was enriched from ~70–95 ¹⁵N atom %, NO₃⁻ ~10–50 ¹⁵N atom %, and NH₄⁺ from ~91–97 ¹⁵N atom %. Samples were sacrificed at 96 h by injecting ZnCl₂ (100 μL of 50% w/v) through the septa to inhibit microbial activity. On the second cruise, a time series experiment was run at all depths at sites 1 and 2. The enrichment was 10 μmol L⁻¹ for each isotope, i.e., the same as that described above for ¹⁵N-N₂O,

with samples being sacrificed at 0, 48, 72, and 96 h by injecting ZnCl₂ (100 μL of 50% w/v) through the septa to inhibit microbial activity.

On return to the laboratory, all of the gas-tight vials were equilibrated to 22°C and a headspace (2 mL analytical grade helium) introduced as above. The vials were then shaken vigorously and rolled, as above, to allow N₂ gas to equilibrate between the water phase and headspace. Samples of the headspace (50 μL) were then injected using an autosampler (Multipurpose Sampler MSP2, Gerstel) into an elemental analyzer (Flash EA 1112, Thermo-Finnigan) interfaced with the continuous flow isotope ratio mass spectrometer (as above). The reduction and oxidation columns in the elemental analyzer are run at 980°C to reduce trace NO and N₂O to N₂, and N₂ and CO₂ are then separated on a GC Poropak column (PoraPLOT Q). The mass spectrometer was calibrated with N₂ in helium over air-equilibrated water at 22°C and the mass charge ratios for *m/z* 28, *m/z* 29, and *m/z* 30 (²⁸N₂, ²⁹N₂, and ³⁰N₂) measured. Precision as a coefficient of variation is better than 1%.

Once each gas-tight vial had been analyzed for ¹⁵N-N₂ gases, the vials were uncapped and the water analyzed for NO₃⁻ and NO₂⁻ (as above). Changes in concentration were then plotted against time and the rate of net production and/or consumption during the incubation derived by linear regression.

Values for production of either ²⁹N₂ or ³⁰N₂ were calculated as excess over that in the references before the addition of ¹⁵N isotopes and then per unit volume according to Thamdrup and Dalsgaard (2000):

$$p \text{ nmol N}_2 \text{ L}^{-1} = \left[\left(\frac{{}^x\text{N}_2}{\sum \text{N}_2} \right)_{\text{sample}} - \left(\frac{{}^x\text{N}_2}{\sum \text{N}_2} \right)_{\text{reference}} \right] (1) \\ \times \sum \text{N}_2_{\text{sample}} \times \alpha^{-1} \times V^{-1}$$

where $p \text{ nmol N}_2 \text{ L}^{-1}$ is the production of either $p^{29}\text{N}_2$ or $p^{30}\text{N}_2$; the fractions ${}^x\text{N}_2/\sum \text{N}_2$ represent the signal ratio for either ${}^{29}\text{N}_2$ or ${}^{30}\text{N}_2$ (${}^x\text{N}_2$) to total signal $\sum \text{N}_2$ (total signal for *m/z* ratios 28, 29, and 30 for either *sample* or *reference*, respectively); α is nmol L⁻¹ per signal; and V the volume of water taken for N₂ analysis. Rates of $p^{29}\text{N}_2$ and $p^{30}\text{N}_2$ production were calculated from linear regression of amount against time. The calculation of an excess amount (pmol) of ⁴⁵N₂O and ⁴⁶N₂O in the 125-mL sample bulb was essentially the same as that above, where α was pmol per signal. Subsequently, the total amount of N₂O produced was calculated according to the volume of gas sampled (125 mL), relative to the headspace (400 mL) and the remainder in the 2-liter flask according to Weiss and Price (1980). Rates of $p^{45}\text{N}_2\text{O}$ and $p^{46}\text{N}_2\text{O}$ production were estimated by dividing total production by 96 h for the incubation period.

Statistical analyses were performed using SPSS v. 13.0. In the majority of cases, the data from different depths were treated as replicates for a particular treatment and any differences between sites 1 and 2 were analyzed using an independent *t*-test. When comparing the means of paired samples, a paired samples *t*-test was used across the data

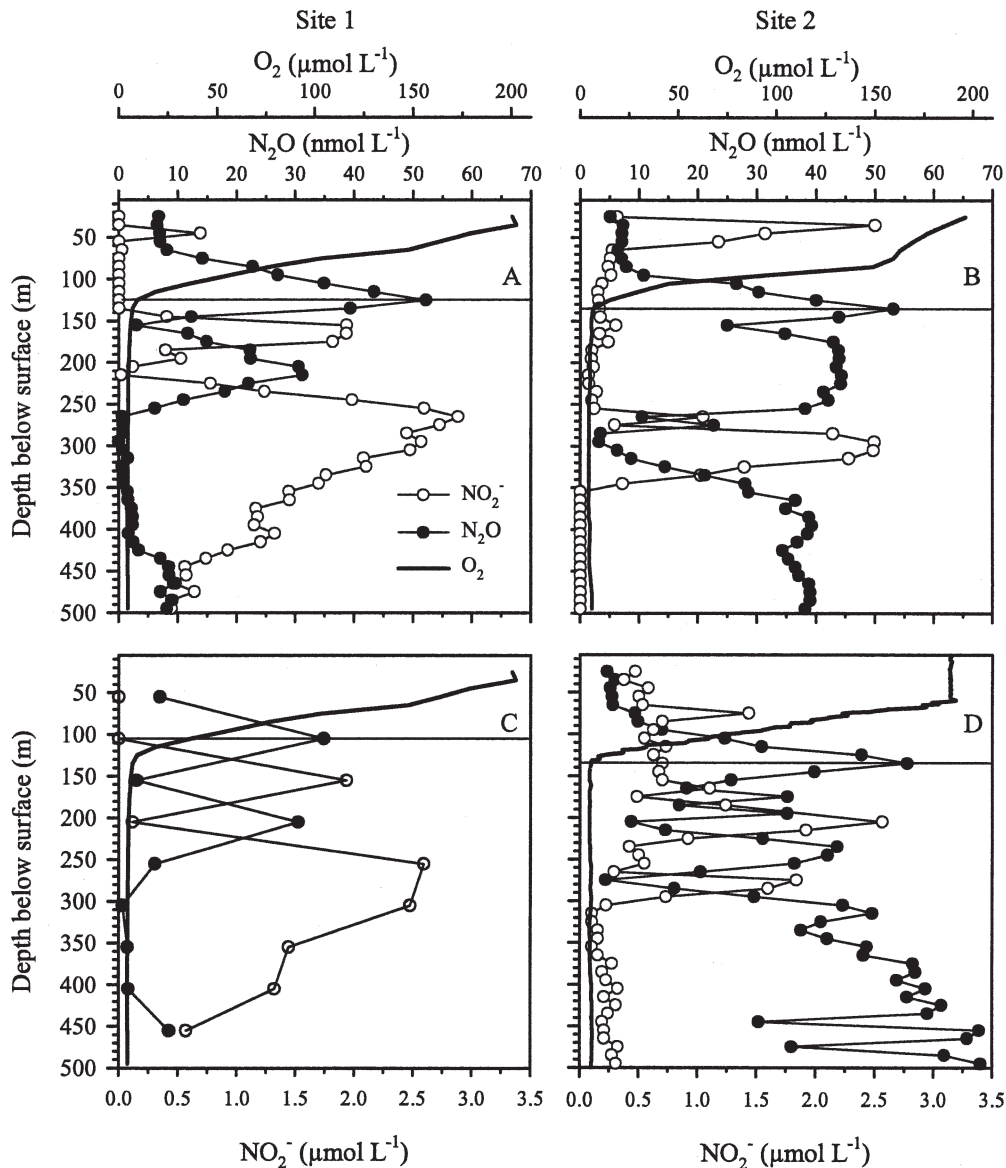


Fig. 1. Water column profiles at 10-m resolution for O_2 , N_2O , and NO_2^- at (A) site 1 and (B) site 2, during the intermonsoon (cruise 2). (C) The data for site 1 in (A) repeated at a 50-m resolution, and (D) water column profiles at 10 m resolution for O_2 , N_2O , and NO_2^- at site 2 during the southwesterly monsoon (cruise 1). Horizontal line indicates the peak in N_2O relative to O_2 concentration.

from both sites, i.e., $n = 8$. Correlations are Pearson's correlation. The alpha value was set at 0.05.

Results

High-resolution water column profiles—During the intermonsoon period in October, oxygen dropped along a linear gradient from 100% of air saturation (4.5 ml L^{-1} , $\sim 198 \mu\text{mol L}^{-1}$) at 35 m, to less than 20% (0.9 ml L^{-1} , $\sim 41 \mu\text{mol L}^{-1}$) by 105 m at both sites (Fig. 1A,B). Beyond 105 m, oxygen saturation decreased logarithmically to approximately 0.1 ml L^{-1} ($\sim 4.5 \mu\text{mol L}^{-1}$) by 165 m, i.e., the detection limit of the oxygen meter. Oxygen was

at or below the detection limit at all the remaining depths at both sites. During the southwesterly monsoon in June, the pattern was similar at site 2 (Fig. 1D), and although, again, oxygen saturation dropped to 0.1 ml L^{-1} ($\sim 4.5 \mu\text{mol L}^{-1}$) by 165 m, the fully oxygenated surface layers extended down to 65 m. Our high-resolution work was focused on the dynamic top 500 m of the water column. Each profile exhibited a clear subsurface peak in NO_2^- at 35–75 m, which coincided with the initial linear decrease in oxygen, after the first inflection. Once into the OMZ, NO_2^- exhibited further clear single or multiple maxima depending on site and season, with a particularly complex structure at site 2 during the monsoon.

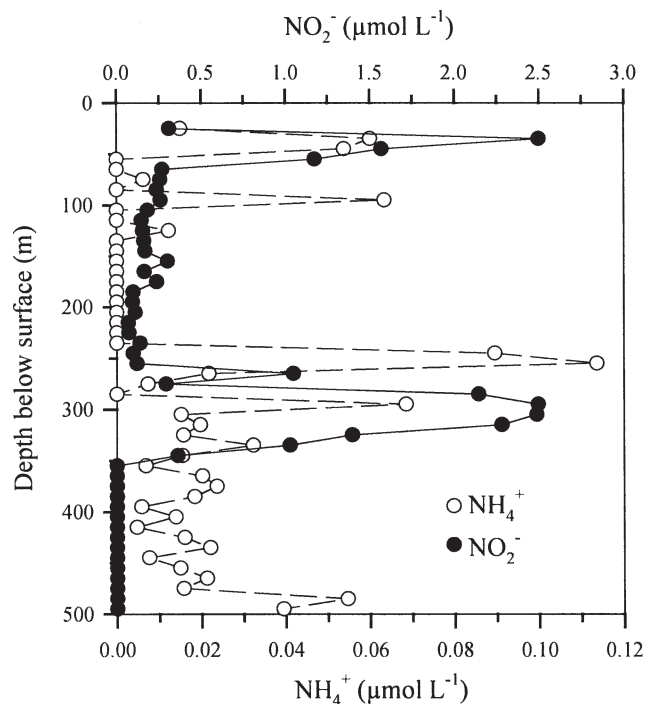


Fig. 2. Water column profiles at 10-m resolution for NH_4^+ and NO_2^- at site 2 during the second cruise.

In the top 50–70 m of water, N_2O was largely at equilibrium with the overlying atmosphere, i.e., 6.5–7 nmol L^{-1} (Fig. 1). Below this, regardless of season or site, N_2O increased to $\sim 52 \text{ nmol L}^{-1}$. This first peak corresponds to the second sharp inflection in oxygen at 125 m (0.2 $\text{mL O}_2 \text{ L}^{-1}$, 8 $\mu\text{mol L}^{-1}$, $\sim 4\%$ saturation) or 135 m (0.14 $\text{O}_2 \text{ mL L}^{-1}$, $\sim 6 \mu\text{mol L}^{-1}$), i.e., what would be considered as the oxic–suboxic interface. Below this depth, and into the OMZ itself, N_2O concentration covaried with NO_2^- , with varying degrees of complexity depending on site and season. For example, at site 1 in October (Fig. 1A), N_2O decreased sharply to 2 nmol L^{-1} at 150 m, as NO_2^- increased. This was followed by an increase in N_2O , to a second peak of 32 nmol L^{-1} at 210 m, while NO_2^- decreased. There was a similar pattern at site 2 in October (Fig. 1B), but, during the monsoon in June, there was more structure in the profile, with multiple covarying peaks and troughs of NO_2^- and N_2O to 300 m (Fig. 1D). Many of the previously published data for water column profiles of N_2O and NO_2^- have a resolution of only 50 to 100 m, and the data at site 1 are repeated at a 50-m resolution for comparison (Fig. 1C). Notice how the first N_2O peak now appears to occur where the O_2 is $\sim 30 \mu\text{mol L}^{-1}$.

Ammonium concentrations were low throughout the water column, i.e., $< 0.11 \mu\text{mol L}^{-1}$, with the majority of data either at, or below, the limit of detection (0.0125 $\mu\text{mol L}^{-1}$) (Fig. 2). There were only two clearly identifiable peaks, i.e., those with not just a single datum point, and these were at 35 and 255 m and, although associated with NO_2^- peaks, the two were not significantly correlated. The average NH_4^+ concentration was 0.03 $\mu\text{mol L}^{-1}$.

^{15}N -isotope incubation experiments, ^{15}N - N_2O —With $^{15}\text{NO}_2^-$ and $^{14}\text{NH}_4^+$, both $^{45}\text{N}_2\text{O}$ and dual-labeled $^{46}\text{N}_2\text{O}$ were produced at all four depths at both sites, with $^{46}\text{N}_2\text{O}$ dominating ($p = 0.004$, $t = 3.187$, $\text{df} = 24$; Fig. 3A,B). With $^{15}\text{NO}_3^-$ and $^{14}\text{NH}_4^+$, both isotopic species were produced in all the incubations, but production was dominated by the single labeled $^{45}\text{N}_2\text{O}$ ($p = 0.001$, $t = 3.729$, $\text{df} = 24$; Fig. 3C,D). With a combination of $^{15}\text{NH}_4^+$, and either $^{14}\text{NO}_2^-$ or $^{14}\text{NO}_3^-$, both single-labeled $^{45}\text{N}_2\text{O}$ and dual-labeled $^{46}\text{N}_2\text{O}$ were produced at 125 m at site 1 (Fig. 3E,G), and both 135 and 155 m at site 2 (Fig. 3F,H). In addition, with $^{15}\text{NH}_4^+$ and $^{14}\text{NO}_2^-$ or $^{14}\text{NO}_3^-$, single labeled $^{45}\text{N}_2\text{O}$ was produced at 165 m and 265 m at site 1 (Fig. 3E,G) and at 265 and 295 m at site 2 (Fig. 3F,H) but not $^{46}\text{N}_2\text{O}$. Overall, with $^{15}\text{NH}_4^+$, production was dominated by $^{45}\text{N}_2\text{O}$ ($p = 0.002, 0.001$, $t = 3.481, 3.966$, $\text{df} = 24$, for NO_2^- and NO_3^- , respectively). In addition, no significant production of ^{15}N - N_2O could be measured at 210 m and 265 m for sites 1 and 2, respectively (Fig. 3E–H).

The data for the predicted (q) and measured distribution of ^{15}N (q') in the ^{15}N - N_2O incubations, with either $^{15}\text{NO}_2^-$ or $^{15}\text{NO}_3^-$, are summarized in Table 1 (see discussion for a full definition of q). In the presence of $^{15}\text{NO}_2^-$, there was no overall significant difference between q and q' , i.e., ^{15}N was binomially distributed in N_2O with respect to the ^{15}N labeling of the NO_2^- pool. With $^{15}\text{NO}_3^-$ though, q' was significantly lower than q ($p < 0.005$) (paired t -test), and ^{15}N was, therefore, not binomially distributed. We identified peaks and troughs in NO_2^- concentration to target with the subsequent ^{15}N isotope incubations. While largely we hit our target with the recast of the CTD for the ^{15}N - N_2 incubations (one cast for four depths), we missed our mark on some occasions collecting water for the ^{15}N - N_2O incubations (two casts for four depths); therefore, the concentrations of ambient NO_2^- at each depth were not identical in the two suites of experiments, although a paired t -test showed them not to be significantly different. Bulk N_2O concentrations were measured in the time series parallel ^{15}N incubations for N_2 and showed no transient build up of N_2O over the 96-h incubation, any changes in the concentration during the incubations were minor (data not shown).

^{15}N -isotope incubation experiments, ^{15}N - N_2 —In the dose response experiment from the first cruise, there was significant ^{15}N - N_2 gas production, with both $^{15}\text{NO}_2^-$ and $^{15}\text{NO}_3^-$ (data not shown). No significant production of either ^{15}N - N_2 gas species could be measured in the presence of $^{15}\text{NH}_4^+$. During the second cruise there was quasilinear production of $^{29}\text{N}_2$ and $^{30}\text{N}_2$ with time in the presence of $^{15}\text{NO}_2^-$ (Fig. 4). The mean rates of $^{29}\text{N}_2$ and $^{30}\text{N}_2$ production were 0.074 $\text{nmol N}_2 \text{ L}^{-1} \text{ h}^{-1}$ (range = 0.013–0.148, mean $r^2 = 0.90$) and 0.046 $\text{nmol N}_2 \text{ L}^{-1} \text{ h}^{-1}$ (range = 0.005–0.141, mean $r^2 = 0.80$), respectively. The mean rate of ^{15}N - N_2 production was therefore 0.083 $\text{nmol N}_2 \text{ L}^{-1} \text{ h}^{-1}$. The rate of $^{29}\text{N}_2$ production was significantly positively correlated with ambient NO_2^- concentration, where NO_2^- concentrations were greater than 0.1 $\mu\text{mol L}^{-1}$ ($r = 0.82$, $p < 0.05$, $n = 7$). The production

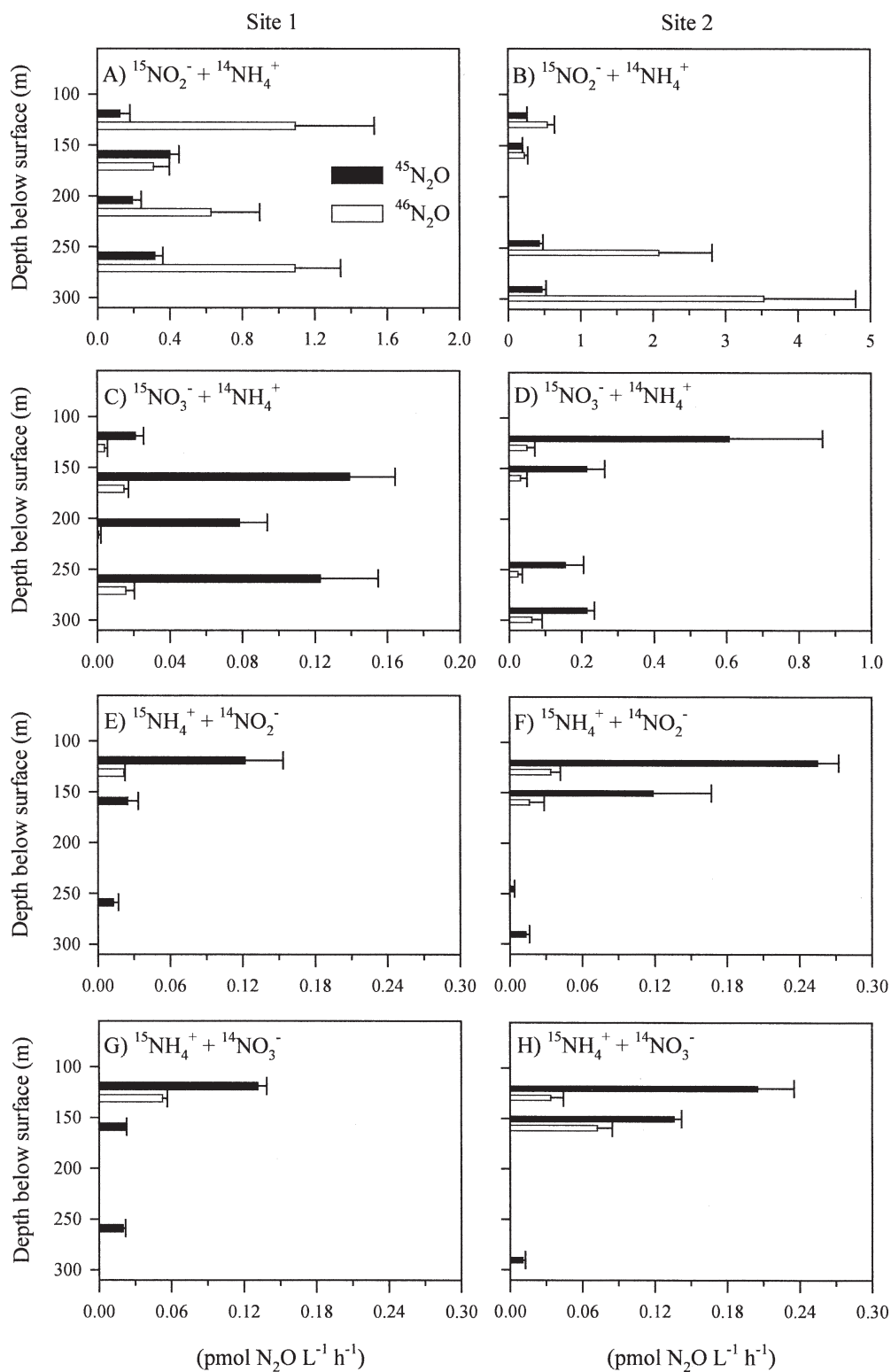


Fig. 3. Net production of single $^{45}\text{N}_2\text{O}$ and dual labeled $^{46}\text{N}_2\text{O}$ at all depths for both sites during the second cruise for (A) and (B) $^{15}\text{NO}_2^- + ^{14}\text{NH}_4^+$ at sites 1 and 2, respectively, (C) and (D) $^{15}\text{NO}_3^- + ^{14}\text{NH}_4^+$ at sites 1 and 2, (E) and (F) $^{15}\text{NH}_4^+ + ^{14}\text{NO}_2^-$ at sites 1 and 2, and (G) and (H) $^{15}\text{NH}_4^+ + ^{14}\text{NO}_3^-$ at sites 1 and 2 (mean \pm SE, $n = 3$). First depths for incubations are from the first N_2O peak at the oxic-suboxic interface.

Table 1. Summary of ^{15}N - N_2O experiments at all depths for both sites during the second cruise, including ambient NO_2^- or NO_3^- (NO_x^-) concentration, rates of NO_2^- accumulation and NO_3^- reduction, ^{15}N -atom (%) labeling, predicted (q) and measured (q') ^{15}N content of N_2O , and any significant difference (paired t -test). Values are the means of three replicate incubations, nd = not determined.

Site, depth (m)	^{15}N labeled pool (NO_x^-)	Ambient NO_x^- ($\mu\text{mol L}^{-1}$)	Rate of NO_2^- accumulation ($\text{nmol L}^{-1} \text{h}^{-1}$)	Rate of NO_3^- reduction ($\text{nmol L}^{-1} \text{h}^{-1}$)	^{15}N atom (%) of NO_x^- pool	Predicted ^{15}N in N_2O produced (q)	Measured ^{15}N in N_2O produced (q')	Mean difference
1, 125	NO_2^-	0.23	1.9	14.9	97	0.97	0.95	
1, 165	NO_2^-	1.12	4.1	28.4	89	0.89	0.61	
1, 210	NO_2^-	1.09	5.4	43.5	89	0.89	0.87	
1, 265	NO_2^-	0.75	2.9	16.0	92	0.92	0.87	
2, 135	NO_2^-	0.16	13.2	19.8	98	0.98	0.81	
2, 155	NO_2^-	0.08	nd	22.8	98	0.98	0.70	
2, 265	NO_2^-	1.55	11.6	18.5	86	0.86	0.91	
2, 295	NO_2^-	2.02	11.0	30.0	83	0.83	0.94	
Mean		0.87		24.23	92	0.92	0.83	0.09
t								1.59
p								0.16
1, 125	NO_3^-	20.66	as above		32	0.32	0.28	
1, 165	NO_3^-	17.45			36	0.36	0.18	
1, 210	NO_3^-	17.37			36	0.36	0.02	
1, 265	NO_3^-	16.66			37	0.37	0.20	
2, 135	NO_3^-	18.03			35	0.35	0.14	
2, 155	NO_3^-	17.20			36	0.36	0.23	
2, 265	NO_3^-	16.79			37	0.37	0.23	
2, 295	NO_3^-	18.26			35	0.35	0.36	
Mean		17.80			36	0.36	0.20	0.16
t								4.05
p								0.005

of $^{29}\text{N}_2$ with time was more consistent than $^{30}\text{N}_2$ in the presence of $^{15}\text{NO}_3^-$. There was measurable production with time of ^{15}N - N_2 gas with $^{15}\text{NH}_4^+$ and $^{14}\text{NO}_2^-$ at some depths at site 2, although, on average, production was 10 times less than the $^{29}\text{N}_2$ produced from analogous incubations with $^{15}\text{NO}_2^-$ (Fig. 4E).

Nitrate reduction and nitrite accumulation—Nitrate was reduced at all depths at both sites at an average rate of $24.23 \text{ nmol L}^{-1} \text{ h}^{-1}$ (Table 1). The rates of NO_3^- reduction were not significantly different between the two sites; however, the rates of NO_2^- accumulation were. On average, at site 1, NO_2^- accumulation could account for 14% of NO_3^- reduction, but a significantly greater proportion at site 2, i.e., 56%.

Discussion

Recognized pathways for N_2O production—Experimental data for either nitrification or denitrification as potential sources of N_2O in the open ocean are scarce (Elkins et al. 1978; Dore and Karl 1996; Castro-González and Farías 2004). Naqvi and Noronha (1991) published profile data at 50- to 100-m resolution in the Arabian Sea (K12: 18°N 69°E), which show a first peak of N_2O of $\sim 40 \text{ nmol L}^{-1}$ within the oxycline at 100 m. In contrast, the 10-m resolution profiles reported here (Fig. 1) identified the first peak in N_2O ($\sim 52 \text{ nmol L}^{-1}$) to occur deeper down at the actual oxic–suboxic interface, i.e., at the second sharp

inflection in oxygen. The interpretation of data like that of Naqvi and Noronha (1991) and the example presented here (Fig. 1C) may have led to the original rationale of high N_2O saturations in low oxygen waters being almost exclusively due to nitrification (see review by Codispoti et al. 1992), though the profiles of Naqvi et al. (1998) agree with our findings.

Evidence for N_2O from the reduction of NO_2^- —The relative proportions of $^{44}\text{N}_2\text{O}$, $^{45}\text{N}_2\text{O}$, and $^{46}\text{N}_2\text{O}$ gas produced from a mixed pool of ^{14}N and ^{15}N can be predicted according to Hauck et al. (1958):

$$[p + q]^2 = p^2 + 2pq + q^2 \quad (2)$$

where p and q are the proportions of ^{14}N and ^{15}N , respectively, in the N substrate pool, $p + q$ is equal to unity, and p^2 , $2pq$, and q^2 are the proportions of $^{44}\text{N}_2\text{O}$, $^{45}\text{N}_2\text{O}$, and $^{46}\text{N}_2\text{O}$, respectively. The $^{15}\text{NO}_2^-$ incubations showed production of ^{15}N - N_2O in a binomial distribution with respect to the ^{15}N labeling of the NO_2^- pool (i.e., $^{14}\text{NO}_2^-$, $p + ^{15}\text{NO}_2^-$, q) at all depths (125 to 295 m) at both sites, i.e., q is not significantly different from q' (Fig. 3 and Table 1). This is very good evidence that the sole reduction of NO_2^- is a source of N_2O in the top 200 m of the OMZ in the Arabian Sea, even at the first N_2O peak at the actual oxic–suboxic interface. With the addition of $^{15}\text{NO}_3^-$, we still recovered ^{15}N labeled N_2O ; however, the ^{15}N was not binomially distributed with respect to the NO_3^- pool (Fig. 3 and Table 1). Although oxygen was recorded at

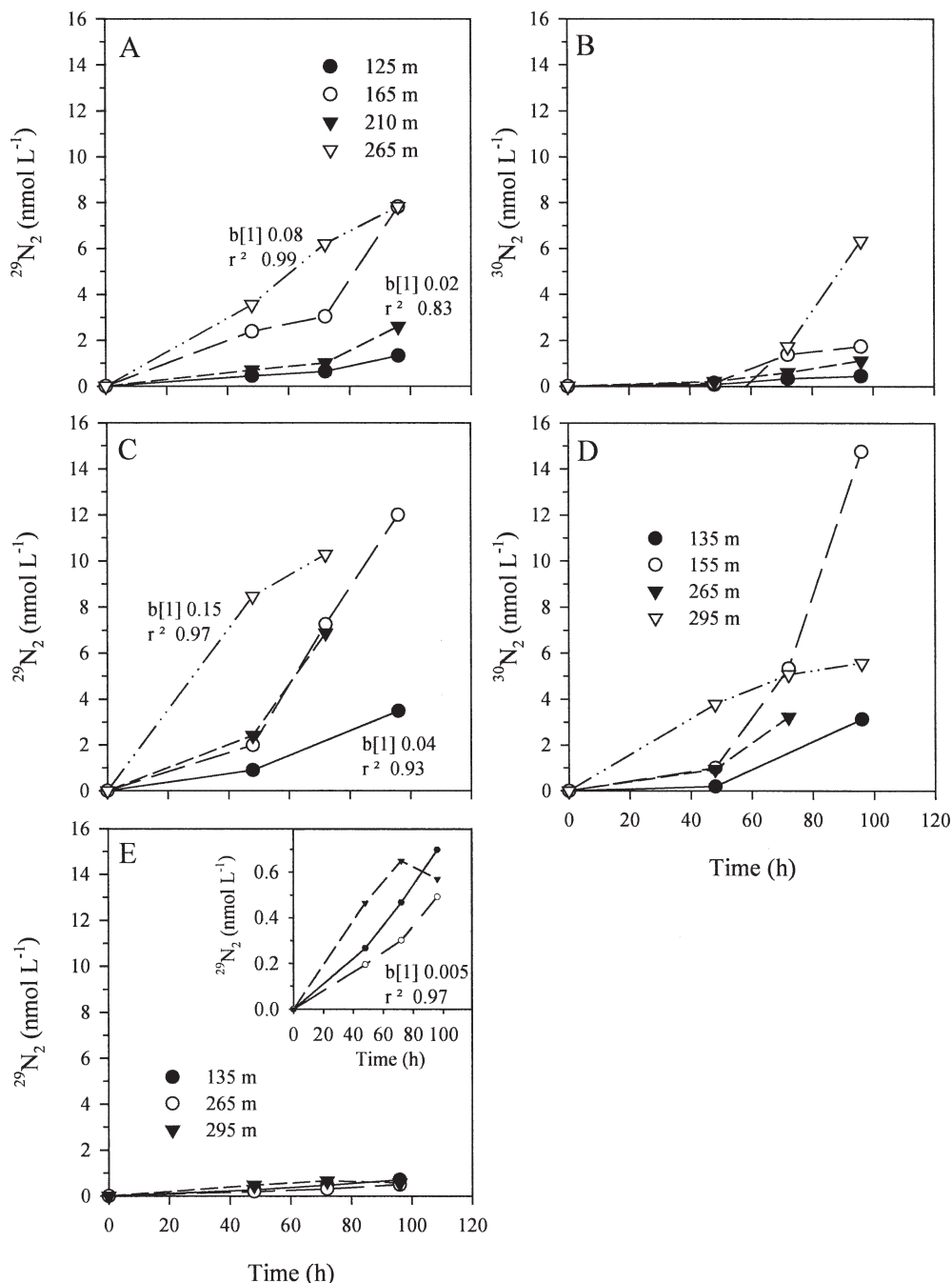


Fig. 4. Production of $^{15}\text{N-N}_2$ gas with $^{15}\text{NO}_2^-$ as a function of time at all depths for both sites during the second cruise for (A) $^{29}\text{N}_2$ and (B) $^{30}\text{N}_2$ for the four depths at site 1, and (C) and (D) the same but at site 2. (E) is the production of $^{29}\text{N}_2$ as a function of time with $^{15}\text{NH}_4^+$ and $^{14}\text{NO}_2^-$ at depths showing linear production at site 2, inset shows the same data on a more appropriate scale. Regression coefficients (r^2 and $b1$, i.e., slope) are included to illustrate the different rates of production (mean, $n = 3$).

0.2 mL $\text{O}_2 \text{ L}^{-1}$ at 125 m at site 1 and 0.14 and 0.13 $\text{O}_2 \text{ mL L}^{-1}$ at 135 m and 155 m, respectively, at site 2, it was at or below the detection limit (0.1 mL L^{-1}) at all the remaining depths at both sites. The production of N_2O from NO_2^- and NO_3^- suggests that oxygen had become sufficiently physiologically limiting to allow NO_3^- and NO_2^- reduction to occur (Körner and Zumft 1989), even at

the upper depths where nitrification was still active (Fig. 3E–H). In the case of the $^{15}\text{NO}_3^-$ additions, no $^{15}\text{NO}_2^-$ was added directly; therefore, assuming that N_2O is derived binomially from the NO_2^- pool (as above), some $^{15}\text{NO}_3^-$ must have been reduced to $^{15}\text{NO}_2^-$ for it to be further reduced to $^{15}\text{N-N}_2\text{O}$. The nutrient data showed not only that NO_3^- was reduced, but also that NO_2^-

accumulated during the incubations (Table 1), supporting the hypothesis of NO_3^- reduction to NO_2^- before reduction to N_2O . Assuming that the movement of both $^{14}\text{NO}_3^-$ and $^{15}\text{NO}_3^-$ into the NO_2^- pool is proportional to their concentrations (a central assumption for the use of isotopes), a revised q was calculated from the amount of NO_3^- potentially reduced in a 96-h period in addition to the starting concentration of ambient $^{14}\text{NO}_2^-$. NO_3^- is reduced first to NO_2^- ; the NO_2^- then accumulates at the ^{15}N ratio of the NO_3^- pool being reduced, which in turn dilutes the ambient pool of $^{14}\text{NO}_2^-$, which would mix with the ambient $^{14}\text{NO}_2^-$ to produce a revised q of the NO_2^- pool according to

$$\text{revised } q_{\text{NO}_2^-} = \frac{\text{NO}_3^- \text{ reduced} \times q_{\text{NO}_3^-}}{\text{totNO}_2^- \text{ pool}} \quad (3)$$

where revised $q_{\text{NO}_2^-}$ is the revised q of the NO_2^- pool, NO_3^- reduced is the amount of NO_3^- reduced in 96 h (calculated from the rate of NO_3^- reduction), $q_{\text{NO}_3^-}$ is the predicted proportion of ^{15}N in the NO_3^- pool, and totNO_2^- pool is the ambient NO_2^- plus the total amount of reduced NO_3^- . The $^{14}\text{NO}_2^-$ and $^{15}\text{NO}_2^-$ are then reduced, as above, to give ^{15}N - N_2O with a distribution that reflects the revised distribution of ^{15}N in the NO_2^- pool, and this scenario is illustrated in Fig. 5A. The figures for revised q (mean = 0.27 SE \pm 0.02) calculated from the measured rates of NO_3^- reduction over 96 h are not significantly different from q' measured in the N_2O pool with $^{15}\text{NO}_3^-$ addition (mean = 0.21 SE \pm 0.04) (paired t -test, $t = -1.38$, $p > 0.05$). Hypothetically, therefore, it is possible that in combination with the ambient NO_2^- , the NO_3^- reduced in 96 h would be able to account for the shift between predicted q and measured q' . Admittedly, this is a simplified scenario, since the q of NO_2^- will be changing throughout the incubation period, yet we have only one measure of q' of N_2O at 96 h.

Logically, if $^{15}\text{NO}_3^-$ can be reduced to, and accumulate as, $^{15}\text{NO}_2^-$ in the $^{15}\text{NO}_3^-$ incubation experiments, ambient $^{14}\text{NO}_3^-$ can also accumulate as $^{14}\text{NO}_2^-$ in the $^{15}\text{NO}_2^-$ incubations, thus diluting the ^{15}N enrichment of the NO_2^- pool (Fig. 5A). However, a paired t -test between the measured q' of the N_2O pool with $^{15}\text{NO}_2^-$ addition (mean = 0.83 SE \pm 0.04) and the revised q of NO_2^- (mean = 0.76 SE \pm 0.03) (from $^{14}\text{NO}_3^-$ reduction, ambient $^{14}\text{NO}_2^-$ and added $^{15}\text{NO}_2^-$) showed no significant difference (paired t -test, $t = 1.46$, $p > 0.05$). This suggests that the reduction of NO_3^- to NO_2^- can explain the distribution of ^{15}N in the N_2O pool with both $^{15}\text{NO}_3^-$ and $^{15}\text{NO}_2^-$ additions. Together, these analyses further support the idea that extracellular NO_2^- is the dominant source of N_2O in the upper OMZ of the Arabian Sea.

The peaks and troughs in N_2O observed in the water column indicate that the production and reduction of N_2O are not occurring at the same rate throughout the water column. If we are arguing that the same process, i.e., the reduction of NO_2^- , is the source of N_2O and potentially N_2 , then this structure may seem counterintuitive, since overall the production of N_2 increased with depth, yet the major peak in N_2O production occurred where the production of

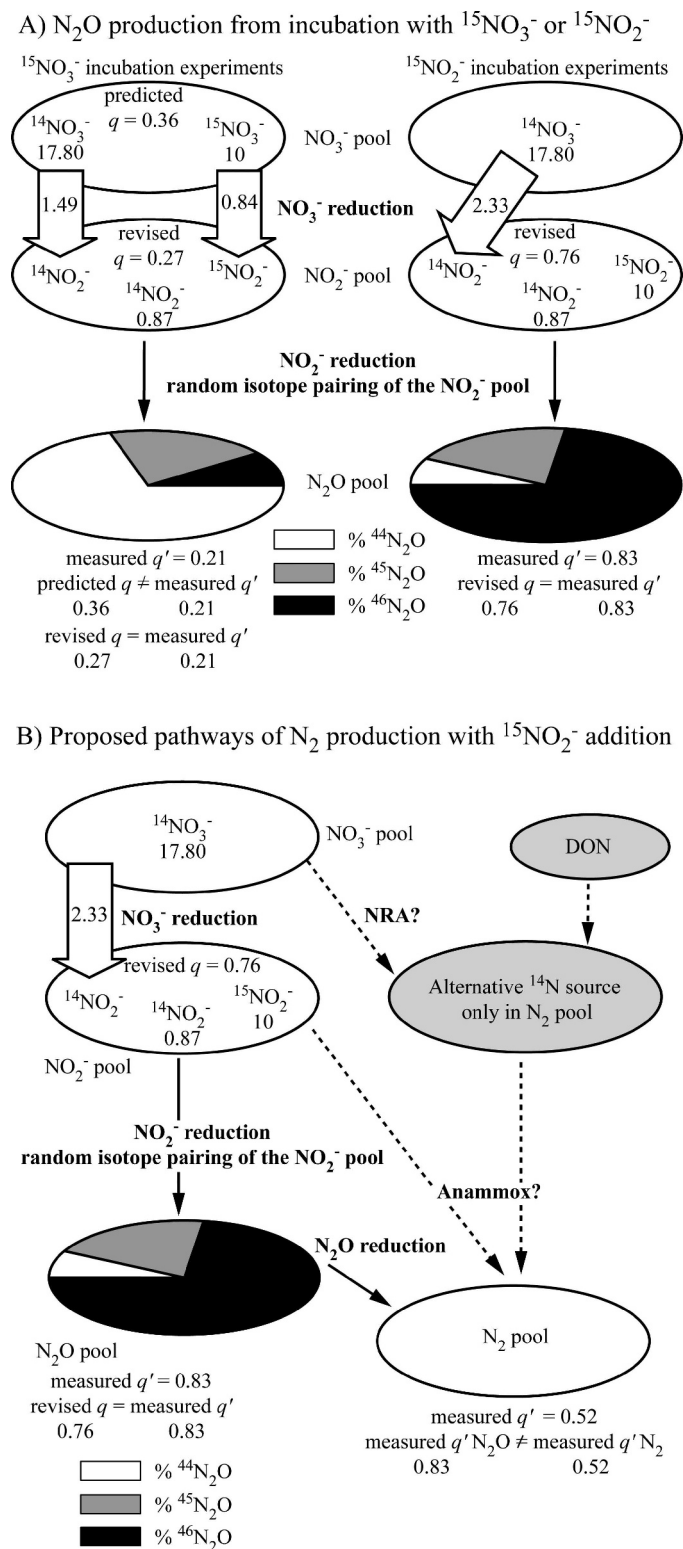


Fig. 5. Theoretical movement of ^{14}N and ^{15}N along dominant pathways from (A) $^{15}\text{NO}_3^-$ or $^{15}\text{NO}_2^-$ additions to N_2O , and (B) production of N_2 from $^{15}\text{NO}_2^-$ addition. Numbers in pools represent concentration in $\mu\text{mol L}^{-1}$; q is the proportion of ^{15}N in the pool; numbers in arrows represent potential concentration of NO_3^- reduced to NO_2^- over 96 h. = represents no significant difference ($p > 0.05$), \neq represents significant difference ($p < 0.05$) (paired t -test). Dashed lines represent hypothesized pathways.

N_2 was lowest, i.e., at the oxic–suboxic interface. However, examination of the ratio of $^{30}\text{N}_2$ produced (Fig. 4B,D, 0.45–14.76 nmol L^{-1}) to $^{46}\text{N}_2\text{O}$ produced (Fig. 3A,B, 0.23–3.53 pmol L^{-1}) (to avoid the problems with the nonbinomially distributed $^{29}\text{N}_2$ with $^{15}\text{NO}_2^-$, see below), after 96 h from the paired N_2 and N_2O incubations on the second cruise, shows that the ratio of N_2 to N_2O produced was not constant throughout the water column. For example, at site 1, where the peaks and troughs in N_2O were most defined, the ratio of N_2 to N_2O produced is lowest where there is a peak in N_2O , namely, 409:1 at 125 m. At the second N_2O peak (210 m), the ratio of N_2 to N_2O produced was 1777:1. In contrast, in the troughs (165 and 265 m) the ratio of N_2 to N_2O produced was, on average, 5668:1, and overall there was a significant negative correlation between the ratio of N_2 to N_2O produced and the ambient concentration of N_2O at site 1 ($r = 0.97$, $p = 0.03$), i.e., where in situ N_2O concentrations were found to be high, there was a relatively low ratio of N_2 to N_2O produced. At site 2, where the peaks and troughs of N_2O were less defined, there was still a very high ratio of N_2 to N_2O produced of 64833:1 at the first trough at 155 m. Ultimately, if the reduction of N_2O to N_2 balanced the reduction of NO_2^- to N_2O , then there would be no net accumulation or peaks in N_2O at all. The same may also be true for the lack of accumulation of NO_2^- at some depths; a trough of NO_2^- does not necessarily mean that NO_3^- is not being reduced to NO_2^- , but that the rate of NO_2^- reduction (or oxidation for nitrification) is equal to, or exceeds, the rate of NO_3^- reduction (Betlach and Tiedje 1981). The expression of the enzymes in the classic denitrification pathway is modulated, to varying degrees, by the presence of oxygen, or by inhibition from reduced products (Körner and Zumft 1989), and, interestingly, N_2O reductase activity has been found to be directly modulated by the presence or absence of oxygen (Moir et al. 1995). We suggest, therefore, certainly at the oxic–suboxic interface, that the peaks of N_2O may be the result of N_2O reductase turning off in response to moderate oxygen (4% of saturation) at the top of the OMZ. Throughout the rest of the water column, modulation of N_2O reductase, by oxygen or another limiting factor, could still generate peaks and troughs in N_2O from the reduction of NO_2^- (Granger and Ward 2003).

Evidence for N_2O from the oxidation of NH_4^+ —Alternatively, it has been suggested that nitrification is the dominant source of N_2O in the ocean (Cohen and Gordon 1979; Dore et al. 1998). In contrast to this, our incubations with $^{15}\text{NH}_4^+$ suggested that nitrification, in the classic sense, i.e., N_2O from NH_4^+ oxidation, plays only a minor part. For example, N_2O formed during nitrification requires two N atoms from the NH_4^+ pool and, with 10 $\mu\text{mol L}^{-1}$ $^{15}\text{NH}_4^+$ and less than 0.015 $\mu\text{mol L}^{-1}$ $^{14}\text{NH}_4^+$, it should be predominantly $^{46}\text{N}_2\text{O}$ (99.7%), yet even at the first N_2O peak $^{45}\text{N}_2\text{O}$ dominated (Fig. 3E–H). The $^{45}\text{N}_2\text{O}$ at the first N_2O peak can most likely be explained by an initial oxidation of $^{15}\text{NH}_4^+$ to $^{15}\text{NO}_2^-$, which was, in turn, reduced to N_2O . This would have enabled $^{15}\text{NO}_2^-$ to combine with ambient $^{14}\text{NO}_2^-$ and

produce $^{45}\text{N}_2\text{O}$ via NO_2^- reduction, along with a smaller amount of $^{46}\text{N}_2\text{O}$ ($2 \times ^{15}\text{NO}_2^-$). In addition, if the oxidation of the NH_4^+ was the direct source of N_2O , then it should not matter whether NO_3^- or NO_2^- were present, yet the production of $^{46}\text{N}_2\text{O}$ was greater in the presence of $^{15}\text{NH}_4^+$ and NO_3^- , compared to $^{15}\text{NH}_4^+$ and NO_2^- (Fig. 3G,H compared to Fig. 3E,F). Any resulting $^{15}\text{NO}_2^-$ from $^{15}\text{NH}_4^+$ would represent proportionally more of the NO_2^- pool when NO_3^- , but not NO_2^- , was added, and the probability of making $^{46}\text{N}_2\text{O}$ would be increased compared to when NO_2^- was added, which is what we found. This suggests that the direct oxidation of $^{15}\text{NH}_4^+$ is not the primary source of N_2O . We cannot, however, fully discount that some of the $^{46}\text{N}_2\text{O}$ may have come from the direct oxidation of $^{15}\text{NH}_4^+$ and, at most, this represented between 2% and 5% of the ^{15}N - N_2O produced directly in the $^{15}\text{NO}_2^-$ incubations at 125 m to 135 m, for site 1 and 2, respectively. Further, the production of ^{15}N - N_2O from $^{15}\text{NH}_4^+$ is important because the moderate amount of oxygen that was present in the water in the upper depths could, potentially, have been depleted during our 24 h acclimatization period, and, hence, we may have inhibited nitrification. The fact that we measured ^{15}N - N_2O from $^{15}\text{NH}_4^+$ suggests that this was not the case, and conditions for N_2O via nitrification should have been optimal (Anderson and Levine 1986). Overall our findings are in agreement with those of Castro-González and Fariás (2004), who concluded that only 8% of the N_2O produced in the OMZ off northern Chile was due to nitrification; though their approach with inhibitors was different from that reported here.

Alternative sources of N_2O production—What was particularly interesting about the $^{15}\text{NH}_4^+$ incubations was the production of just $^{45}\text{N}_2\text{O}$ (in terms of ^{15}N) at some depths below 165 m (Fig. 3E–H). The sole production of $^{45}\text{N}_2\text{O}$ can only be explained by a pairing of a ^{14}N and ^{15}N atom, potentially coupling the reduction of NO_2^- to the oxidation of NH_4^+ , with N_2O being formed as gaseous end-product, e.g., $4\text{HNO}_2 + 2\text{NH}_3 \rightarrow 3\text{N}_2\text{O} + 5\text{H}_2\text{O}$. Bock et al. (1995) reported the formation of N_2O from *Nitrosomonas* under oxygen limitation in the presence of NH_4^+ and NO_2^- . The stoichiometry of this potential reaction suggests that with ^{15}N labeling of the NH_4^+ pool, ^{15}N -labeled N_2O could be produced as either $1 \times ^{46}\text{N}_2\text{O} + 2 \times ^{44}\text{N}_2\text{O}$ or $2 \times ^{45}\text{N}_2\text{O} + 1 \times ^{44}\text{N}_2\text{O}$. Our data, which showed production of only $^{45}\text{N}_2\text{O}$ at some depths, suggest that the latter is the most likely. Though this is direct evidence for a novel pathway for the formation of N_2O in the Arabian Sea, the amounts, as before with the oxidation of $^{15}\text{NH}_4^+$ to $^{46}\text{N}_2\text{O}$ at 125 m and 135 m, were very small, i.e., 0.1–2% of that produced with $^{15}\text{NO}_2^-$. In turn, some of the $^{45}\text{N}_2\text{O}$ at the top two depths could also be attributed to this process. There is, however, an alternative explanation for the formation of N_2O from NH_4^+ . Naqvi and Noronha (1991) postulated that nitrification could be coupled to denitrification through NO, e.g., $\text{NH}_4^+ \rightarrow \text{NO} \rightarrow \text{N}_2\text{O}$, whereby nitrification supplies NO under oxygen limitation and denitrification reduces the NO to N_2O . While data for the distribution of NO in the ocean are scarce, Ward and

Zafiriou (1988) did show NO maxima in the eastern tropical North Pacific at the boundaries of the denitrification zone. Here, partial nitrification of $^{15}\text{NH}_4^+$ could have generated ^{15}NO , if ^{14}NO were present in the water column, as would seem likely, then the reduction of these two species would produce a predominance of $^{45}\text{N}_2\text{O}$. For this to be possible at the depths below 165 m, however, would require nitrifying bacteria to be able to scavenge O_2 deep in the OMZ.

Fate of N_2O —Despite the significant production of N_2O from NO_2^- at all depths throughout the water column, the N_2O has the potential to be reduced (Fig. 1, Fig. 5), and it is likely that the vast majority of N_2O produced at depth is reduced to N_2 (Cohen and Gordon 1978; Elkins et al. 1978). For example, the N_2O coming up from below 500 m was completely reduced between 250 and 350 m at site 1 and, potentially, only the N_2O produced at the oxic–suboxic interface (125–135 m) would ever reach the atmosphere. Indeed, the production and dominance of $^{15}\text{N}-\text{N}_2$ (Fig. 4) in our incubations dictates that this is the case, but it does not appear to be a straightforward turnover of the ambient N_2O pool. If the source of N_2O for reduction to N_2 were extracellular N_2O , we would expect, at the rates of $^{15}\text{N}-\text{N}_2$ production (0.01–0.20 nmol $^{15}\text{N}-\text{N}_2 \text{ L}^{-1} \text{ h}^{-1}$) (Fig. 4) measured, the ambient pool of N_2O (average 25 nmol L^{-1}) in the water to have been substantially turned over during the 96 h $^{15}\text{N}-\text{N}_2\text{O}$ incubations (if not completely at some depths). However, the vast majority of N_2O measured at the end of the incubation was still $^{44}\text{N}_2\text{O}$, i.e., the ambient N_2O was not significantly turned over. This corroborates the minor changes in bulk N_2O concentrations measured in the parallel N_2 incubations (data not shown). Therefore, we conclude that the measured production of $^{15}\text{N}_2$ represents an almost exclusively intracellular reduction of $^{15}\text{NO}_2^-$ to $^{15}\text{N}-\text{N}_2\text{O}$ and, in turn, $^{15}\text{N}_2$. Hence, our measured production of $^{15}\text{N}-\text{N}_2\text{O}$ in the water column (Fig. 3) represents only that either leaked (i.e., $^{15}\text{NO}_2^- \rightarrow ^{15}\text{N}-\text{N}_2\text{O} \rightarrow ^{15}\text{N}_2$) or that released as a final product (i.e., $^{15}\text{NO}_2^- \rightarrow ^{15}\text{N}-\text{N}_2\text{O}$) into the water. Though, in order to generate the troughs in N_2O concentration (Fig. 1), the ambient N_2O pool must be turned over eventually, but this is comparatively slow.

N_2 production—The production of $^{15}\text{N}-\text{N}_2$ was approximately linear throughout the incubations, with r^2 values for all but two of the incubations exceeding 0.8 (Fig. 4). Although there was possibly a tendency for increasing $^{30}\text{N}_2$ production, the results did not suggest any major bottle effect on the rates, such as occasionally observed in a previous study (Kuypers et al. 2005). The rates of $^{15}\text{N}-\text{N}_2$ gas production reported here (0.01–0.20 nmol $^{15}\text{N}-\text{N}_2 \text{ L}^{-1} \text{ h}^{-1}$) are lower than those reported by Dalsgaard et al. (2003) and Kuypers et al. (2005) for other oxygen minimum zones of the global ocean. Nevertheless, the production of $^{15}\text{N}-\text{N}_2$ gas does help to rationalize the overall loss of NO_2^- from the Arabian Sea, but, as discussed below, it may not be due solely to denitrification, as postulated widely in the past, or anammox, as we currently understand it (Naqvi 1987; Thamdrup and Dalsgaard 2002; Trimmer et al. 2003).

If denitrification were the sole source of N_2O and N_2 , then in the presence of $^{15}\text{NO}_3^-$ and assuming steady state, the proportions of $^{44}\text{N}_2\text{O}$, $^{45}\text{N}_2\text{O}$, and $^{46}\text{N}_2\text{O}$ would match the proportions of $^{28}\text{N}_2$, $^{29}\text{N}_2$, and $^{30}\text{N}_2$ (Trimmer et al. 2006). For simplicity, any disturbance in the relative proportions of the ^{15}N labeled gases can be represented by comparing the percentage of ^{15}N gas that is either $^{29}\text{N}_2$ or $^{45}\text{N}_2\text{O}$, i.e., $(^{29}\text{N}_2 / (^{29}\text{N}_2 + ^{30}\text{N}_2)) \times 100$, or $(^{45}\text{N}_2\text{O} / (^{45}\text{N}_2\text{O} + ^{46}\text{N}_2\text{O})) \times 100$. These percentages are calculated from the production of $^{15}\text{N}-\text{N}_2$ or $^{15}\text{N}-\text{N}_2\text{O}$ at 96 h, and therefore any potential nonlinearity of the N_2 data is no longer relevant. In the presence of $^{15}\text{NO}_2^-$, the percentage of $^{15}\text{N}_2$ gas as $^{29}\text{N}_2$ was, on average, 64% (70% at site 1 and 58% at site 2) and, for $^{45}\text{N}_2\text{O}$, 27% (28% at site 1 and 27% at site 2). This difference indicates that not all of the N_2 is from the same source as the N_2O , but our scenario with $^{15}\text{NO}_2^-$ is a little more complex. Assuming that there is a single source of both N_2 and N_2O , then on the addition of $^{15}\text{NO}_2^-$ any N_2O and N_2 produced will represent the q (i.e., proportion ^{15}N) of the NO_2^- at that point. As the experiment progresses, not only will the ^{15}N in the NO_2^- pool be turned over, but it will also be diluted by the ^{14}N from $^{14}\text{NO}_3^-$ being reduced to NO_2^- (as discussed above), and the q of the NO_2^- pool will decrease. The N_2 pool will reflect the cumulative effect of all of the ^{14}N and ^{15}N turned over from the start of the incubation. The extracellular, measurable N_2O pool, however, is also likely to reflect the cumulative effect of all the ^{14}N and ^{15}N , since the turnover of N_2O in this pool would be slow enough to be insignificant in terms of the incubation. Therefore, at the end of the experiment, the percentage of ^{15}N as $^{29}\text{N}_2$ would match the percentage of ^{15}N as $^{45}\text{N}_2\text{O}$, despite a changing distribution of ^{15}N in the NO_2^- throughout the incubation. The fact that the percentage of ^{15}N as $^{29}\text{N}_2$ gas was always higher than the $^{45}\text{N}_2\text{O}$ gas indicates that not all of the N_2 is from the same source as the N_2O .

Although a small proportion of N_2O could be ascribed to nitrification at the top of the OMZ, and, by implication, NO_2^- , it was not enough to significantly affect the binomial distribution of ^{15}N in the N_2O . Since N_2O is an intermediate to N_2 in the denitrification pathway, and any N_2O from nitrification could be reduced to N_2 , if nitrification is not a significant source of N_2O then it follows that it is also not a significant source of N_2 . Shaw et al. (2006) reported an average yield of 0.26% N_2O per mole of NO_2^- for seven nitrifying bacteria, and we used this to estimate the contribution of NO_2^- from nitrification. Our maximum production of N_2O with $^{15}\text{NH}_4^+ + ^{14}\text{NO}_3^-$ of 0.20 pmol $\text{L}^{-1} \text{ h}^{-1}$ would be equivalent to 78 pmol $\text{NO}_2^- \text{ L}^{-1} \text{ h}^{-1}$, which is equivalent to only 0.3% of the measured rates of NO_3^- reduction. It is unlikely, therefore, that the contribution of NO_2^- from nitrification could affect the predicted binomial distribution of ^{15}N in the N_2O or N_2 at the top of the OMZ.

Nitrification cannot account for the imbalance between the percentage of ^{15}N as $^{29}\text{N}_2$ and $^{45}\text{N}_2\text{O}$ with $^{15}\text{NO}_2^-$. In addition, in the presence of $^{15}\text{NO}_2^-$, it cannot be due to ^{14}N from NO_3^- being reduced to NO_2^- , since this would cause deviation from the binomial distribution of ^{15}N in the N_2O relative to the NO_2^- pool, as discussed above. The relative

imbalance of percentage ^{15}N as $^{29}\text{N}_2$ to $^{45}\text{N}_2\text{O}$ therefore cannot be explained if denitrification is the only source of N_2 . It is this excess of $^{29}\text{N}_2$ that is indicative of an anammox-like reaction and not classic denitrification (Thamdrup and Dalsgaard 2002). In our previous papers on the measurement of anammox in estuarine sediments we have, as have others, stipulated that the only definitive proof for anammox is the production of $^{29}\text{N}_2$ from $^{15}\text{NH}_4^+$ with either $^{14}\text{NO}_3^-$ or $^{14}\text{NO}_2^-$ under anaerobic conditions (Thamdrup and Dalsgaard 2002; Trimmer et al. 2003). The data reported here are at odds with that stipulation, since we measured very little production of $^{29}\text{N}_2$ in only a few of our $^{15}\text{NH}_4^+$ incubations (Fig. 4E). Linear production of $^{29}\text{N}_2$ with $^{15}\text{NH}_4^+$ was found at only three depths and only at site 2 in the core of the OMZ, but it was small, i.e., 10% of the $^{29}\text{N}_2$ production in the analogous incubations with $^{15}\text{NO}_2^-$ and $^{14}\text{NH}_4^+$, and could not, as such, account for the $^{29}\text{N}_2$ imbalance measured in the incubations with $^{15}\text{NO}_2^-$. This suggests a source of $^{29}\text{N}_2$ (and potentially $^{28}\text{N}_2$) that only contributes to the N_2 pool, i.e., a specific pairing of a ^{15}N from $^{15}\text{NO}_2^-$ and a ^{14}N from an alternative source that does not appear to be the extracellular NH_4^+ pool (Fig. 5B). Potentially, this could be ^{14}N supplied from the dissolved organic nitrogen pool, which has largely been ignored (Sanders and Jickells 2000), or NH_4^+ from dissimilatory or assimilatory reduction of NO_3^- or NO_2^- (Rees et al. 1999; Allen et al. 2002).

References

- ALLEN, A. E., M. H. HOWARD-JONES, M. G. BOOTH, M. E. FRISCHER, P. G. VERITY, D. A. BRONK, AND M. P. SANDERSON. 2002. Importance of heterotrophic bacterial assimilation of ammonium and nitrate in the Barents Sea during summer. *J. Mar. Syst.* **38**: 93–108.
- ANDERSON, I. C., AND J. S. LEVINE. 1986. Relative rates of nitric oxide and nitrous oxide production by nitrifiers, denitrifiers and nitrate respirers. *Appl. Environ. Microbiol.* **51**: 938–945.
- BETLACH, M. R., AND J. M. TIEDJE. 1981. Kinetic explanation for accumulation of nitrite, nitric oxide and nitrous oxide during bacterial denitrification. *Appl. Environ. Microbiol.* **42**: 1074–1084.
- BOCK, E., I. SCHMIDT, R. STÜVEN, AND D. ZART. 1995. Nitrogen loss caused by denitrifying *Nitrosomonas* cells using ammonium or hydrogen as electron donors and nitrite as electron acceptor. *Arch. Microbiol.* **163**: 16–20.
- BRETTAR, I., AND G. RHEINHEIMER. 1992. Influence of carbon availability on denitrification in the central Baltic Sea. *Limnol. Oceanogr.* **37**: 1146–1163.
- CASTRO-GONZÁLEZ, M., AND L. FARIÁS. 2004. N_2O cycling at the core of the oxygen minimum zone off northern Chile. *Mar. Ecol. Prog. Ser.* **280**: 1–11.
- CODISPOTI, L. A., AND J. P. CHRISTENSEN. 1985. Nitrification, denitrification and nitrous oxide cycling in the eastern tropical South Pacific Ocean. *Mar. Chem.* **16**: 277–300.
- , J. W. ELKINS, T. YOSHINARI, G. E. FRIEDERICH, C. M. SAKAMOTO, AND T. T. PACKARD. 1992. On the nitrous oxide flux from productive regions that contain low oxygen waters, p. 271–284. *In* B. N. Desai [ed.], *Oceanography of the Indian Ocean*. Oxford and IBH Publishers.
- , AND T. T. PACKARD. 1980. Denitrification rates in the eastern tropical South Pacific. *J. Mar. Res.* **38**: 453–477.
- COHEN, Y., AND L. I. GORDON. 1978. Nitrous oxide in the oxygen minimum zone of the eastern tropical North Pacific: Evidence for its consumption during denitrification and possible mechanisms for its production. *Deep-Sea Res.* **25**: 509–524.
- , AND ———. 1979. Nitrous oxide production in the ocean. *J. Geophys. Res. Oceans Atmos.* **84**: 347–353.
- DALSGAARD, T., D. E. CANFIELD, J. PETERSEN, B. THAMDRUP, AND J. ACUNA-GONZÁLEZ. 2003. N_2 production by the anammox reaction in the anoxic water column of Golfo Dulce, Costa Rica. *Nature* **422**: 606–608.
- , B. THAMDRUP, AND D. E. CANFIELD. 2005. Anaerobic ammonium oxidation (anammox) in the marine environment. *Res. Microbiol.* **156**: 457–464.
- DEUSER, W. G., E. H. ROSS, AND Z. J. MŁODZINSKA. 1978. Evidence for and rate of denitrification in the Arabian Sea. *Deep-Sea Res.* **25**: 431–445.
- DORE, J. E., AND D. M. KARL. 1996. Nitrification in the euphotic zone as a source for nitrite, nitrate and nitrous oxide at station ALOHA. *Limnol. Oceanogr.* **41**: 1619–1628.
- , B. N. POPP, D. M. KARL, AND F. J. SANSONE. 1998. A large source of atmospheric nitrous oxide from subtropical North Pacific surface waters. *Nature* **396**: 63–66.
- ELKINS, J. W., S. C. WOFSEY, M. B. McELROY, C. E. KOLB, AND W. A. KAPLAN. 1978. Aquatic sources and sinks for nitrous oxide. *Nature* **275**: 602–606.
- GOERING, J. J., AND R. C. DUGDALE. 1966. Denitrification rates in an island bay in the Equatorial Pacific Ocean. *Science* **154**: 505–506.
- GRANGER, J., AND B. B. WARD. 2003. Accumulation of nitrogen oxides in copper-limited cultures of denitrifying bacteria. *Limnol. Oceanogr.* **48**: 313–318.
- HAUCK, R. D., S. W. MELSTED, AND P. E. YANKWICH. 1958. Use of N-isotope distribution in nitrogen gas in the study of denitrification. *Soil Sci.* **86**: 287–291.
- HOLMES, R. M., A. AMINOT, R. KEROUÉL, B. A. HOOKER, AND B. J. PETERSON. 1999. A simple and precise method for measuring ammonium in marine and freshwater ecosystems. *Can. J. Fish. Aquat. Sci.* **56**: 1801–1808.
- HYNES, R. K., AND R. KNOWLES. 1978. Production of nitrous oxide by *Nitrosomonas europaea*: Effects of acetylene, pH, and oxygen. *Can. J. Microbiol.* **30**: 1397–1404.
- KIM, K. R., AND H. CRAIG. 1990. Two-isotope characterisation of N_2O in the Pacific Ocean and constraints on its origin in deep water. *Nature* **347**: 58–61.
- KIRKWOOD, D. S. 1996. Nutrients: Practical notes on their determination in seawater. *Techniques in marine environmental science* No. 17. ICES.
- KÖRNER, H., AND W. G. ZUMFT. 1989. Expression of denitrification enzymes in response to the dissolved oxygen level and respiratory substrate in continuous culture of *Pseudomonas stutzeri*. *Appl. Environ. Microbiol.* **55**: 1670–1676.
- KUYPERS, M. M. M., AND OTHERS. 2003. Anaerobic ammonium oxidation by anammox bacteria in the Black Sea. *Nature* **422**: 608–611.
- , AND OTHERS. 2005. Massive nitrogen loss from the Benguela upwelling system through anaerobic ammonium oxidation. *Proc. Natl. Acad. Sci. USA* **102**: 6478–6483.
- LAW, C. S., AND N. J. P. OWENS. 1990. Significant flux of atmospheric nitrous oxide from the northwest Indian Ocean. *Nature* **346**: 826–828.
- MOIR, J. W. B., D. J. RICHARDSON, AND S. J. FERGUSON. 1995. The expression of redox proteins of denitrification in *Thiosphaera pantotropha* grown with oxygen, nitrate, and nitrous oxide as electron acceptors. *Arch. Microbiol.* **164**: 43–49.

- MORRISON, J. M., AND OTHERS. 1999. The oxygen minimum zone in the Arabian Sea during 1995. *Deep-Sea Res. II* **46**: 1903–1931.
- NAQVI, S. W. A. 1987. Some aspects of the oxygen deficient conditions and denitrification in the Arabian Sea. *J. Mar. Res.* **45**: 1049–1072.
- , AND R. J. NORONHA. 1991. Nitrous oxide in the Arabian Sea. *Deep-Sea Res.* **38**: 871–890.
- , AND OTHERS. 1998. Budgetary and biogeochemical implications of N₂O isotope signatures in the Arabian Sea. *Nature* **394**: 462–464.
- REES, A., M. WOODWARD, AND I. JOINT. 1999. Measurement of nitrate and ammonium uptake at ambient concentrations in oligotrophic waters of the North-East Atlantic Ocean. *Mar. Ecol. Prog. Ser.* **187**: 295–300.
- SANDERS, R., AND T. JICKELLS. 2000. Total organic nutrients in Drake Passage. *Deep-Sea Res. I* **47**: 997–1014.
- SHAW, L. J., G. W. NICOL, Z. SMITH, J. FEAR, J. I. PROSSER, AND E. M. BAGGS. 2006. *Nitrosospira* spp. can produce nitrous oxide via a nitrifier denitrification pathway. *Environ. Microbiol.* **8**: 214–222.
- STEIN, L. Y., AND Y. L. YUNG. 2003. Production, isotopic composition, and atmospheric fate of biologically produced nitrous oxide. *Annu. Rev. Earth Plant. Sci.* **31**: 329–356.
- THAMDRUP, B., AND T. DALSGAARD. 2000. The fate of ammonium in anoxic manganese oxide-rich marine sediment. *Geochim. Cosmochim. Acta* **64**: 4157–4164.
- , AND ———. 2002. Production of N₂ through anaerobic ammonium oxidation coupled to nitrate reduction in marine sediments. *Appl. Environ. Microbiol.* **68**: 1312–1318.
- TIEDJE, J. M. 1988. Ecology of denitrification and dissimilatory nitrate reduction to ammonium, p. 179–244. *In* A. J. B. Zehnder [ed.], *Biology of anaerobic microorganisms*. John Wiley & Sons.
- TRIMMER, M., J. C. NICHOLLS, AND B. DEFLANDRE. 2003. Anaerobic ammonium oxidation measured in sediments along the Thames Estuary, UK. *Appl. Environ. Microbiol.* **69**: 6447–6454.
- , N. RISGAARD-PETERSEN, J. C. NICHOLLS, AND P. ENGSTRÖM. 2006. Direct measurement of anaerobic ammonium oxidation (anammox) and denitrification in intact sediment cores. *Mar. Ecol. Prog. Ser.* **326**: 37–47.
- UPSTILL-GODDARD, R. C., A. P. REES, AND N. J. P. OWENS. 1996. Simultaneous high-precision measurements of methane and nitrous oxide in water and seawater by single phase equilibration gas chromatography. *Deep-Sea Res. I* **43**: 1669–1682.
- WADA, E., AND A. HATTORI. 1972. Nitrite distribution and nitrate reduction in deep sea waters. *Deep-Sea Res.* **19**: 123–132.
- WARD, B. B., AND O. C. ZAFIRIOU. 1988. Nitrification and nitric oxide in the oxygen minimum of the eastern tropical North Pacific. *Deep-Sea Res.* **35**: 1127–1142.
- WEISS, R. F., AND B. A. PRICE. 1980. Nitrous oxide solubility in water and seawater. *Mar. Chem.* **8**: 347–359.
- YOSHIDA, N. 1988. ¹⁵N-depleted N₂O as a product of nitrification. *Nature* **335**: 528–529.
- , AND OTHERS. 1989. Nitrification rates and ¹⁵N abundances of N₂O and NO₃⁻ in the western North Pacific. *Nature* **342**: 895–897.

Received: 22 January 2006

Accepted: 15 August 2006

Amended: 16 August 2006